Morphological Reconstruction and Ordering in Films of Sphere-Forming Block Copolymers on Striped Chemically Patterned Surfaces

Sang-Min Park, Gordon S. W. Craig, Young-Hye La, and Paul F. Nealey*

Department of Chemical and Biological Engineering, University of Wisconsin—Madison, Madison, Wisconsin 53706

Received May 7, 2008; Revised Manuscript Received September 11, 2008

ABSTRACT: The morphology of thin films of sphere-forming block copolymers on striped chemically patterned surfaces was investigated as a function of thickness and commensurability of the pattern period (L_s) and the lattice spacing of the spherical structure (L_o), using scanning electron microscopy and atomic force microscopy. In all cases, a linear wetting layer forms on the chemical pattern. As the film thickness increases from 10 to 25 nm, protuberances in the wetting layer appear. In 57 nm thick films, when L_s and L_o are sufficiently commensurate, the protuberances in the knurled, linear wetting domain and the spheres in the overlying layer of P(S-*b*-MMA) coordinate during equilibration, resulting in an ordered hexagonal array of partial spherical domains. The range of commensurability over which such an ordered hexagonal structure is achieved decreases when the film thickness is increased to 70 nm. In general, the process leads to a pattern transformation from a series of parallel lines at the substrate surface to an ordered, hexagonal array of spots at the free surface of the film as the block copolymer starts to reconstruct its bulk morphology away from the chemically patterned surface.

Introduction

Block copolymers in thin films (sub-100 nm) can self-assemble into a panoply of scientifically interesting and potentially useful structures.[1−9] These thin film structures typically mimic the thermodynamically preferred morphologies of the bulk copolymer.[10,11] However, equilibrium structures that do not occur in the bulk can form in a thin film as the block copolymer reconstructs its morphology near the surfaces of the film.[12] A relatively simple example of surface reconstruction was provided by Liu et al., who demonstrated a lamellar interface layer in a thin film of cylinder-forming block copolymer on a chemically homogeneous surface.[13] Segalman et al. reported a similar lamellar brush layer at the interface between a thin film of sphere-forming block copolymer and a chemically homogeneous, topographically patterned substrate.[14] Research by Radzilowski et al.[15] and Knoll et al.[12] showed that surface reconstruction of the domains in thin films of cylinder-forming block copolymers on a chemically homogeneous surface led to a variety of structures, such as perforated lamellae, undulating cylinders, and spherical nodules. Additionally, Konrad et al. showed that cylindrical domains can assume a very tortuous, three-dimensional (3D) structure in films on chemically homogeneous substrates as the film thickness was increased beyond a first layer of cylinders adjacent to the substrate.[16] Xu et al. used selective solvent swelling to induce surface reconstruction of cylinder-forming block copolymers to yield ordered, vertically oriented nanopores.[17]

Previously, we have investigated the surface reconstruction of block copolymers as they equilibrate on chemically patterned surfaces. In the case of lamellae-forming block copolymers, we have shown that the same molecular weight block copolymer will form lamellae of different dimensions as it equilibrates in the presence of chemically nanopatterned surfaces of varying pattern periods, with a mismatch of the obtained lamellar spacing versus the bulk lamellar spacing of as much as 10%.[18] In the case of cylinder-forming block copolymers, we demonstrated that a cylindrical morphology could be transformed from a hexagonal arrangement to a square array when the block copolymer equilibrated in the presence of a chemical pattern consisting of a square array of spots.[19] We observed the presence of 3D structures such as loop cylinders and semicylinders as the distance from the chemical pattern interface was increased and the morphology began to reconstruct its bulk morphology. Other research found that scientifically interesting and potentially useful bicontinuous morphologies were created when a symmetric block copolymer that forms lamellae in the bulk equilibrated in the presence of a surface pattern of a square array of circles.[20] The preceding three examples investigated the morphologies created when the underlying chemical nanopattern ranged from a near match to a complete mismatch of the bulk morphology of the block copolymer. Here we examine the morphology of thin films of sphere-forming block copolymers on striped chemically patterned surfaces as a function of film thickness (t) and commensurability of the pattern period (L_s) with the lattice spacing of the spherical structure (L_o). The different blocks of the copolymer selectively wet alternating regions of the pattern, as seen before in the directed assembly of block copolymer domains by chemical nanopatterns.[21] The linear wetting layer contained a series of protuberances that formed a knurled structure in the wetting layer. As t increased, a layer of spherical domains formed above the wetting layer, and aligned with the wetting layer in a hexagonal array, resulting in a pattern transformation from a series of parallel lines at the substrate surface to an ordered, hexagonal array of spots at the free surface of the film.

Experimental Section

Materials. Hydroxyl-terminated polystyrene brush polymer (PS-OH) (M_n = 9.5 kg/mol, PDI = 1.04) and polystyrene-*block*-poly(methyl methacrylate) copolymer (P(S-*b*-MMA)) (M_n = 123 kg/mol for PS and M_n = 35 kg/mol for PMMA, PDI: 1.09) were purchased from Polymer Source, Inc., and used without further purification. The P(S-*b*-MMA) had 80 vol % PS and 20 vol % PMMA, resulting in a bulk morphology that consisted of PMMA spheres in a PS matrix. The PMMA photoresist used for extreme ultraviolet interference lithography (EUV-IL) had M_n = 950 kg/

* To whom correspondence should be addressed: E-mail nealey@engr.wisc.edu; Tel 608-265-8171; Fax 608-262-5434.

10.1021/ma801039v CCC: $40.75
Published on Web 11/04/2008

mol and was purchased from Microchem Corp. Toluene and chlorobenzene were purchased from Aldrich Chemical Co. of Milwaukee, WI.

Sample Preparation. The general process for directed assembly was performed as described previously.[18] The first step in the process is the formation of the chemical pattern. A thin layer of PS-OH was spin-coated from 1.5 wt % toluene solution onto a silicon wafer freshly cleaned with Piranha solution (*caution*!), and then the substrates were annealed under vacuum at 160 °C for 48 h to graft the PS-OH to the silicon substrates and form a PS brush. Ungrafted PS-OH was extracted by repeated rinses with warm toluene. The resulting thickness of the PS brush layer was about 7 nm. A 60 nm thick film of PMMA photoresist was spin-coated on the PS brush anchored to the substrate and baked at 160 °C for 60 s. Extreme ultraviolet interference lithography (EUV-IL) with a transmission membrane grating was used to make line-and-space patterns with periods (L_s) ranging from 50.0 to 60.0 nm, in increments of 2.5 nm. For developing, the exposed photoresist was submerged in a 1:3 mixture of methyl isobutyl ketone and isopropyl alcohol for 30 s at room temperature, rinsed with isopropyl alcohol, and dried in a stream of nitrogen. The lithographically patterned structures in the photoresist were chemically transferred into the PS brush layer by an oxygen plasma treatment. The oxygen plasma was generated in a Plasma Etch, Inc., PE-200 running at 100 W with an O_2 flow rate of 8 cm^3/min. The duration of the plasma was 10 s at room temperature. Subsequent removal of the remaining photoresist yielded a chemical pattern consisting of an array of alternating stripes of untreated and oxygen-plasma-treated PS brush. The dimension of the patterned area was approximately 30 μm by 400 μm.

P(S-*b*-MMA) films were spin-coated onto the chemical patterns from toluene solutions. Spin speed and spin-coating solution concentration were controlled to yield uniform films with controlled thicknesses of 10, 25, 57, or 70 nm. The deposited polymer films on the chemical patterns were annealed under vacuum at 190 °C for 3 days to form the thermodynamically equilibrated morphology. The P(S-*b*-MMA) films were irradiated with UV light (254 nm wavelength at 1 mJ/cm^2) and washed with 97% acetic acid to remove selectively the PMMA block. For the sake of comparison, 57 nm thick P(S-*b*-MMA) films were also coated on chemically homogeneous substrates consisting of native oxide on a silicon wafer.

Analysis. The resulting morphologies were imaged without any metal deposition, using a field emission scanning electron microscope (SEM) (LEO-1550 VP) with an acceleration voltage of 1 kV, a 4 mm working distance, and an in-lens detector under high vacuum. SEM's were analyzed by both in-house image analysis software and fast Fourier transforms (FFT). Atomic force microscopy (AFM) measurements were performed using a Nanoscope III MultiMode AFM from Digital Instruments in the tapping mode. A triangular cantilever made of silicon with a 10 nm end radius was used (MikroMasch) in the AFM. The film thicknesses were verified by ellipsometry (Rudolph Research AutoEL-II).

Results and Discussion

The process for the investigation of the morphology of the sphere-forming P(S-*b*-MMA) on the striped chemical pattern, shown in Figure 1a, proceeded analogously to previous research on the directed assembly of cylinder- and lamellae-forming block copolymers.[22] A striped chemical pattern with L_s set to one of a set of specific, desired values near L_o was generated in a PS-OH brush layer and subsequently spin-coated with a thin film of P(S-*b*-MMA). Upon annealing, the morphology of the block copolymer equilibrated in the presence of the striped chemical pattern to form a complex structure that depended both on t and the commensurability of L_s with L_o. An idealized schematic of the final, equilibrated structure is shown in Figure 1a for the case of a film with $t = L_s = L_o$. At the chemical pattern interface, the PMMA wets the oxidized stripes in the chemical pattern to form a series of knurled, linear domains.

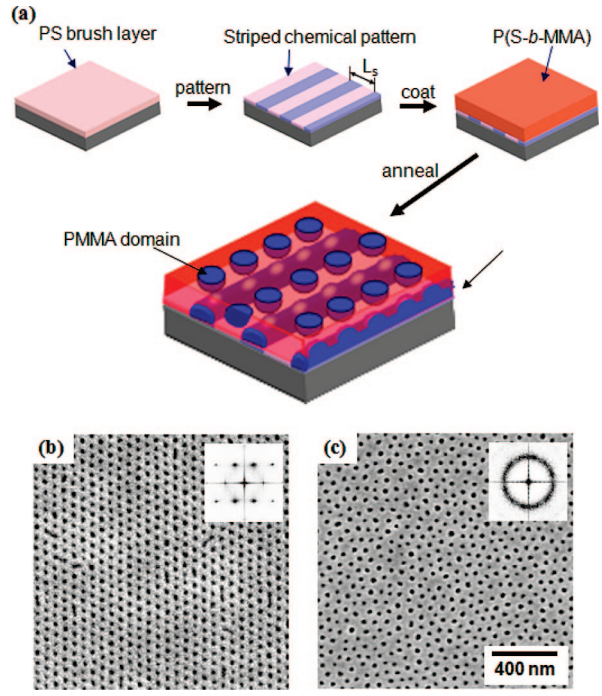

Figure 1. Directed assembly of sphere-forming P(S-*b*-MMA) on a striped chemical pattern. (a) Schematic representation of procedure used to direct the assembly of P(S-*b*-MMA). The image shows the case when the film thickness is approximately equal to the bulk lattice spacing of the spherical domains. The final step in the process schematic is enlarged to show the detail of the assembled structure. Knurled linear domains of PMMA are formed as the wetting layer on the chemically striped pattern. Hexagonal arrays of PMMA domains are formed over the linear domains at the interface, separated by the PS matrix. At this film thickness, the PMMA domains at the free surface appear as hemispherical structures. (b) SEM image of a 57 nm thick film of P(S-*b*-MMA) assembled on a striped chemical pattern (L_s is 57.5 nm). (c) SEM image of a 57 nm thick film of P(S-*b*-MMA) on a chemically homogeneous surface. 2D fast Fourier transform images are inset in both images. The scale bar in (c) applies to both SEM images.

At the free surface of the film, hemispherical domains of PMMA form between the knurled linear domains, generating a hexagonal array of hemispheres.

The idealized structure presented in Figure 1a was experimentally examined with a 57 nm thick film of P(S-*b*-MMA) on a striped chemical nanopattern with $L_s = 57.5$ nm. The resulting plan-view SEM image of the free surface of the film showed an array of PMMA domains that appeared as dark, uniform spots that formed hexagonal arrays over the entire area of the chemical pattern, as seen in Figure 1b. Although we refer to these PMMA structures as spherical domains, we recognize that these domains could have been elliptical or otherwise misshapen and probably were only partial spheres in 57 nm thick films due to the fact that $t \approx L_o$ and that part of the PMMA material in the film resided in the wetting layer.[23] Matching the process scheme shown in Figure 1a, the spherical domains assembled in rows that ran top to bottom in the SEM image, in the same direction as the underlying chemical pattern. In the FFT image in the inset of Figure 1b, sharp peaks in a hexagonal arrangement also confirmed the lateral order of the spherical domains. We determined from analysis of the FFT image that the distance between rows of spherical domains parallel to the underlying striped patterns was the same as L_s in this case.

The effect of the chemical pattern on the assembly of the P(S-*b*-MMA) morphology can clearly be seen in the contrast between the assembled morphology on a striped chemical pattern (Figure 1b) and the self-assembled morphology of the P(S-*b*-MMA) on a chemically homogeneous substrate (Figure

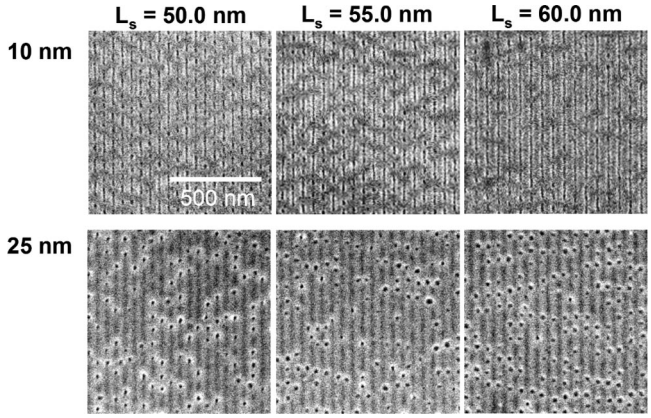

Figure 2. Results of directed assembly of 10 and 25 nm thick films of sphere-forming P(S-*b*-MMA) on striped chemical patterns with varying pattern period, L_s (L_s = 50.0, 55.0, and 60.0 nm). In 10 nm thick films the P(S-*b*-MMA) is ordered with the underlying chemically striped patterns. Primitive spheres begin to form above the aligned wetting layer in 25 nm thick films.

1c). In both cases, discrete, PMMA domains were surrounded by the PS matrix block. On the chemically homogeneous surface, the spherical domains typically had six nearest neighbors, but they lacked long-range hexagonal order, and the corresponding FFT image exhibited a ring pattern, providing further indication of the lack of order in the sample. The average distance between spherical domains on the chemically homogeneous surface (a_o) was 65.2 nm, and the lattice spacing, L_o, of the spherical structure was $a_o\sqrt{3}/2 = 56.3$ nm. The average domain diameter was 26.5 nm.

To investigate how the equilibrated morphology transitions from the knurled, linear structure at the chemical pattern interface to the overlying layer of spherical domains, we prepared and imaged samples with film thicknesses of 10 and 25 nm (both $<L_o/2$) on chemically striped patterns with L_s values of 50, 55, and 60 nm, as shown in the SEM images in Figure 2. In the 10 nm thick films, the PMMA domains selectively wetted the oxidized stripes of the PS brush, as seen before with directed assembly of P(S-*b*-MMA) on chemical nanopatterns made from a PS brush.[22] At the free surface of the 10 nm thick films, a mixture of dots and lines were formed by the PMMA phase. Because the 10 nm film thickness was less than half the bulk sphere diameter of 26.5 nm, we assume that these dots and lines were portions of the PMMA wetting layer that were 10 nm thick. The PMMA wetting layer could not propagate uniformly to the surface because of the significant difference between the percentage of PMMA in the block copolymer (20%) and the percentage of the chemical pattern surface area that had affinity for PMMA (50%).

In the 25 nm thick films the PMMA domains wetting the linear stripes of the chemical pattern were visible as hazy, gray lines, and a number of solid, black, circular PMMA domains aligned with the wetting layer were also evident. AFM analysis revealed that the hazy, linear PMMA phase seen in the SEM did not appear in the phase mode image (see Supporting Information), which was evidence that the linear PMMA domain at the interface did not extend through the thickness of the film to the free surface of the 25 nm thick film. In the height mode of the AFM image, the P(S-*b*-MMA) film on the chemically patterned area had no terrace structures, such as the islands or holes that Yokoyama et al.[9] observed in thin block copolymer films on uniform, chemically homogeneous substrates. In the case of the films presented here, the height difference between the PMMA spheres and the PS matrix region was less than ~2 nm.

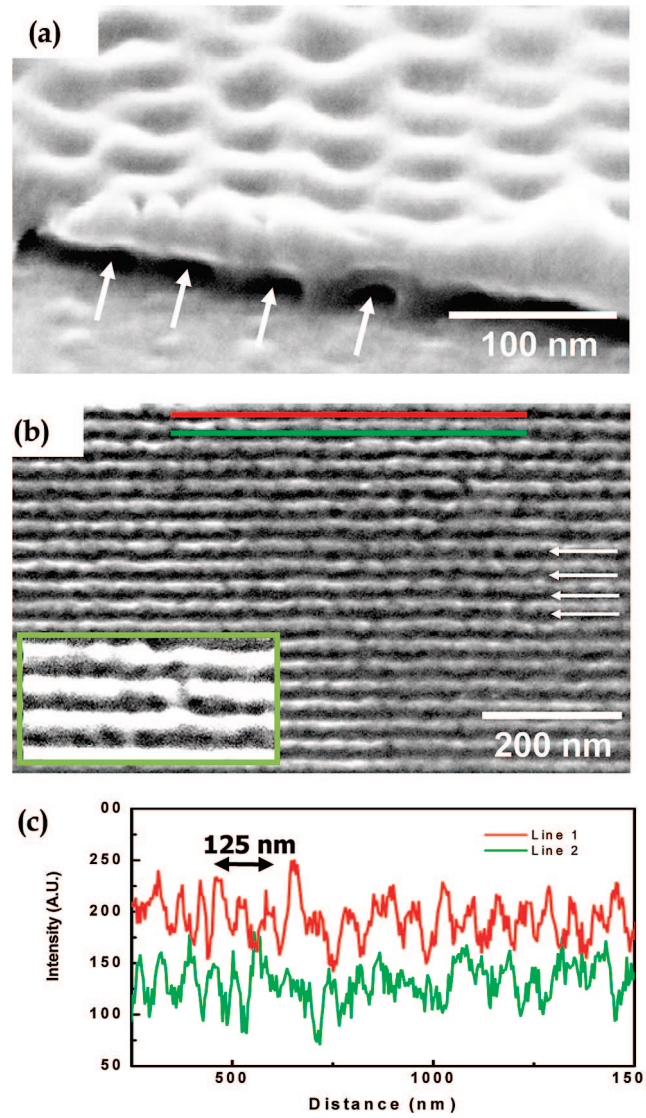

Figure 3. SEM images of results of directed assembly of sphere-forming P(S-*b*-MMA) on striped chemical patterns after selective removal of the PMMA phase. (a) 70° tilted SEM image of a 57 nm thick film. The arrows indicate the wetting layer on the chemical pattern. (b) Backside image of detached film from substrate. The inset in the lower left corner provides a magnified view of the brightness profile observed in the space left behind when the PMMA wetting layer was removed. (c) Brightness profile of red and green lines in (b).

To investigate further the morphology of the sphere-forming P(S-*b*-MMA) at the chemical pattern interface, we imaged the side view of a sharply cleaved, assembled copolymer film. Figure 3a shows the 70° tilted SEM image of a 57 nm thick film of P(S-*b*-MMA) on a striped chemical pattern (L_s = 57.5 nm) after selective removal of the PMMA block. The arrows indicate the cross-sectioned openings in the PS matrix where PMMA wetting layers were present in the film. Above the interfacial wetting layer, there was an uneven PS matrix with hexagonally arranged dimples positioned corresponding to the location of the removed PMMA domains.

We also observed the structure of the P(S-*b*-MMA) film at the chemical pattern interface, as shown in Figure 3b, by peeling the film off the substrate. The detached copolymer film was collected onto a silicon wafer upside down and imaged with SEM. The white arrows show the direction of the stripes of the chemical pattern. The dark region indicates the regions formerly occupied by PMMA, and the bright region indicates the PS matrix. It is evident that the bottom layer near the substrate

formed a continuously aligned wetting layer in the 57 nm thick film. We also produced image brightness profiles of the removed PMMA region in Figure 3b, which we used to determine the general shape of the PMMA wetting layer. The red and green lines in Figure 3b indicate the examined region, and Figure 3c shows the brightness profiles of the corresponding lines. The image brightness profile was an oscillating pattern, indicative of regions in the wetting layer with varying thickness. The wavelength of the oscillation in the brightness profile was ~64 nm, very similar to the spacing of spheres in the bulk block copolymer. Although the height variation of the image brightness profile was unknown, the profile showed that the top surface of the PMMA wetting layer had protuberances, or knurls, in a regular sequence. Also, the knurls along one line were offset from the knurls along a neighboring line, similar to how the spheres in neighboring lines in a hexagonal array are offset from each other. This offset in the knurls suggested that the knurls in adjacent wetting layers of PMMA communicated with each other via the overlying layer of spherical domains. Such a knurled, linear domain structure has not been previously reported in the bulk state, although similar structures have been observed in very thin films of cylinder-forming block copolymers.[12,15]

As the film thickness was increased to 57 nm, which was $\sim L_o$, the films were sufficiently thick for a separate layer of well-ordered, spherical domains to form, as seen in Figure 4. As stated above, given that the $t \approx L_o$ and that a portion of the PMMA in the film resided in the wetting layer at the chemical interface, it is likely that the spherical domains at the surface of the film were hemispheres or portions of a sphere. Each of the 57 nm thick films showed some degree of hexagonal order, as seen by the hexagonal arrangement of the dots in the corresponding FFTs. However, the samples with $L_s < L_o$ had more defects, especially when $L_s = 50$ nm. Also, when $L_s = 50$ nm, the domain spacing (L) determined from FFT equaled L_o, whereas the values of L for the other 57 nm thick films were approximately equal to L_s of each sample. The fact that $L = L_o$ when $L_s = 50$ nm indicated that at this spacing the chemical pattern was ineffective at directing the assembly of the overlying layer of spheres, and the domain spacing reverted back to its bulk value. In contrast, for the samples with $L_s > 50$ nm, the chemical pattern could direct the spherical domains to assemble with the same spacing as the chemical pattern. Interestingly, when $L_s > L_o$ (57.5 and 60 nm), two spacings were determined by FFT. One spacing was in the direction of the chemical pattern lines and matched L_o. The other spacing was in the direction perpendicular to the chemical pattern lines and matched L_s. In short, the spherical domains retained their bulk spacing in the same direction as the lines of the chemical pattern, but the spacing between each line of spheres matched the chemical pattern spacing.

Increasing the film thickness to 70 nm ($\sim 1.25L_o$) led to an overall decrease of order, especially when $L_s < L_o$, as seen in the SEM images and corresponding FFT plots shown in Figure 4. For the 70 nm thick films with $L_s = 50$ or 52.5 nm, the FFT of the SEM image showed a broad, featureless ring, indicative of a lack of hexagonal order in the sample. When $L_s = 50$ nm, the sphere spacing was $\sim L_o = 56.3$ nm, but when $L_s = 52.5$ nm, the sphere spacing was closer to L_s for the sample. FFT plots of the other 70 nm thick films retained a hexagonal array of spots, but the spots were broader than in the FFT plots of the corresponding 57 nm thick films, and a precursor ring was also present. Because the film thickness of the 70 nm thick films was only $1.25L_o$ and because the wetting layer had a thickness between 10 and 25 nm, we expect that the spherical domains in the 70 nm films were complete spheres, and not partial spheres, as we assumed was the case in the 57 nm thick films. It is worth noting that even though both the 57 and 70 nm thick films imaged only the layer of spherical domains immediately above the wetting layer, the layer of spherical domains in the 57 nm thick films had more order than the layer of spherical domains in the 70 nm thick films. One possible explanation for this decrease in order in the 70 nm thick films is that it is easier for the morphology to form with hemispheres at the free surface ($t = 57$ nm) than to have complete or nearly complete spheres tangent to or immediately below the free surface ($t = 70$ nm). Previous work has pointed to the energetic penalty associated with the deformation of the interpenetrating corona chains that uniformly fill the matrix space between spheres in the bulk.[24]

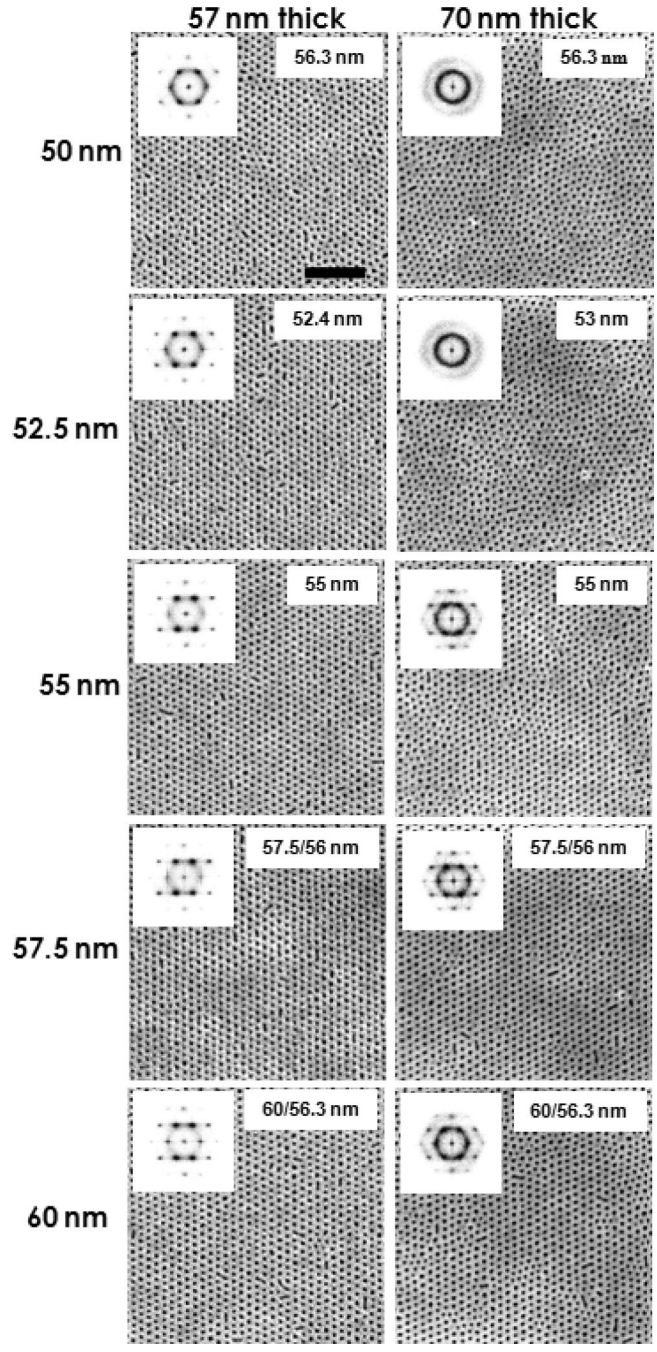

Figure 4. SEM images of 57 and 70 nm thick films of P(S-*b*-MMA) that were directed to assemble on striped chemical patterns with L_s values listed on the left. Fewer defects and improved order were seen in the case when the polymer chains were extended beyond their bulk state compared to the case when they were compressed from their bulk state. The 400 nm scale bar in the top left image applies to all images. An FFT of each SEM image is provided in the inset. Spacing(s) determined from FFT are shown above each FFT.

In the case of a complete sphere tangent to the free surface, there would be an energetic penalty associated with the significant deformation of the corona chains adjacent to where the sphere and the free surface contact. Analogous effects have been observed with half-cylinders and cylinders at the free surface of thin films.[25]

Along with film thickness, the commensurability between L_s and L_o played a role in the degree of order of the equilibrated morphology. Even in 25 nm thick films (Figure 2), the role of pattern/copolymer period commensurability can be seen. The position of the black spheres in the 25 nm thick films was strongly dependent on the periodicity of the chemically striped patterns. When L_s was 55 or 60 nm, the percentage of spherical domains located between the dark gray PMMA wetting layers was 89% or 97%, respectively. In contrast, only 3% of the spherical domains were found between the PMMA wetting layers when L_s was 50.0 nm. The remaining 97% of the spherical domains were located directly above the aligned PMMA wetting layers. It was surprising to us that such a small difference in periodicity could lead to such a significant change in the location of the domains in the sample. One possible explanation for the location of the PMMA domains above the PMMA wetting region in the 25 nm thick sample with $L_s = 50$ nm could be that there was insufficient space in the compressed geometry for distinct domains to form, and instead the domains seen in the SEM were necking up from the wetting layer. Another possible explanation is that in the compressed conformation with $L_s < L_o$ a chain conformation was induced that led to the relocation of the sphere position above the PMMA wetting layers.

The commensurability between L_s and L_o also had an effect on the ordering and spacing of the spherical domains in 57 and 70 nm thick films, as seen in Figure 4. For the 57 nm thick films, even though all of the equilibrated morphologies contained hexagonal arrays of spheres at the free surface, the P(S-*b*-MMA) film on the $L_s = 50.0$ nm pattern had spheres whose order possessed a greater number of defect structures than was present in the other 57 nm thick films. A comparison of 57 nm thick films on substrates with $L_s = 52.5$ and 60.0 nm, which had an approximately equal deviation of their L_s values from L_o, reveals that the $L_s = 52.5$ nm sample, which contained polymer chains compressed from their bulk state, had more defects than the $L_s = 60.0$ nm sample, which contained polymer chains extended from their bulk state. Similarly, for the 70 nm thick films, the sample with $L_s = 55$ nm had less order, as evidenced by the thicker ring in the FFT, than the sample with $L_s = 57.5$ nm.

A likely explanation for the asymmetry in the effect of incommensurability can be found in a phenomenological model for the equilibration of a block copolymer film in the presence of a chemical nanopattern. Cheng et al. have shown a simple, thermodynamic model for spherical domains[26] that is similar to earlier models applied to lamellae.[18,27] At the core of these models, and for models of block copolymer phase separation in general,[10] is the balance of the domain−domain interface energy and the elastic energy associated with extending or compressing the polymer chains. The free energy associated with the elastic energy of the polymer chain scales with L_s^2, whereas the free energy associated with the domain−domain interface which scales with $1/L_s$.[27,28] The difference in dependence on L_s of these two competing effects leads to a greater energetic penalty when $L_s < L_o$ than when $L_s > L_o$. This energetic penalty must be overcome by the energy supplied by the chemical pattern for the chemical pattern to induce an ordered structure in the overlaying film. The energy supplied by the chemical pattern is relatively independent of L_s,[18] and thus the chemical pattern is less able to induce an ordered domain structure when $L_s < L_o$ than when $L_s > L_o$. Similar asymmetry was observed in the topographically directed assembly of spherical microdomains[26] and the chemical pattern induced assembly of cylindrical domains.[29]

The physical processes that lead to the formation at equilibrium of the knurled, linear structure at the interface and the well-ordered layers of spherical domains farther away from the interface can be inferred from the images shown in Figures 2 and 3. As known from previous work on directed assembly with chemical patterns,[21,30,31] the PMMA block wets the oxidized stripes of the chemical pattern. As seen before in previous studies investigating the reconstruction of block copolymer morphologies on chemically patterned substrates,[19,20,32] as the distance from the chemically patterned interface is increased, the block copolymer will reconstruct its bulk morphology, which in the work presented here was spherical domains. As seen in Figure 4, such spherical domains formed within L_o of the surface. The PMMA wetting layer at the interface must equilibrate with the overlying layer of spherical domains. As seen in Figure 3, equilibration resulted in the formation of knurls in the wetting layer, and these knurls were offset from each other in neighboring stripes on the chemical pattern, such that they aligned with the hexagonally ordered spherical domains above them.

Theoretically, stacking the layers of hexagonally ordered spheres directly above the knurls in the linear wetting layer was not favored energetically because in a hexagonally close packed (HCP) structure, there are two sets of interstitial sites for the location of one hexagonal array of spheres directly on top of another hexagonal array of spheres.[9,33] Therefore, in multilayered spherical block copolymer domains, either poor in-plane order or cubic arrays of spherical domains are often observed, while long-range layered structures are maintained in the film thickness direction.[9,24,33] The knurled, linear structure can be considered as a hybrid of spherical and cylindrical structures. Therefore, the two sets of possible location sites normally available in a three-dimensional HCP matrix were not available in the knurled layer, and as a result, there was only one favored route for the simultaneous equilibration of the overlying hexagonal array of spheres and the underlying knurled, linear structure on the striped chemical pattern.

Conclusion

Much of the previous research on block copolymer films directed to assemble on chemical patterns involved domains that assembled vertically and continuously away from a chemical pattern that approximately matched the geometry of the bulk morphology of the block copolymer. In contrast, the work presented here demonstrates that one can use directed assembly on a chemical pattern to arrive at a markedly different pattern at the free surface of the film, without having domains at the free surface that are connected to the wetting layer on the chemical pattern. In effect, the interplay between the striped chemical pattern and the spherical bulk structure of the block copolymer, as the block copolymer equilibrates and reaches its lowest energy state in the presence of the chemically patterned surface, creates a type of 3D assembly technique. The end result of the equilibration is a geometric transformation of a pattern, going from a one-dimensional pattern (a series of lines) on the substrate to a two-dimensional pattern (an ordered array of spots) on the surface of the thin film. Beyond providing an example of geometric pattern transformation and the surface reconstruction of a sphere-forming block copolymer, this research also demonstrates the communication between adjacent minority block wetting layers via an overlying hexagonal array of spherical domains. Because the method relies solely on the equilibration of the block copolymer with the underlying chemically patterned substrate, and not on any chemical

transformations within the block copolymer, the method should be applicable to a broad array of sphere-forming block copolymers.

Acknowledgment. This work was supported by the Semiconductor Research Corporation (SRC) (2005-MJ-985) and the National Science Foundation through the Nanoscale Science and Engineering Center (DMR-0425880). This work was based upon research conducted at the Synchrotron Radiation Center, University of Wisconsin—Madison, which is supported by the NSF under Award DMR-0537588.

Supporting Information Available: AFM images of a 25 nm thick film of sphere-forming P(S-*b*-MMA) assembled on a linear chemical pattern with $L_s = 60$ nm. This material is available free of charge via the Internet at http://pubs.acs.org.

References and Notes

(1) Cheng, J. Y.; Ross, C. A.; Smith, H. I.; Thomas, E. L. *Adv. Mater.* **2006**, *18*, 2505.
(2) Hawker, C. J.; Russell, T. P. *MRS Bull.* **2005**, *30*, 952.
(3) Nealey, P. F.; Edwards, E. W.; Müller, M.; Stoykovich, M. P.; Solak, H. H.; De Pablo, J. J. *IEEE Tech. Dig. IEDM* **2005**, 356.
(4) Park, C.; Cheng, J. Y.; Fasolka, M. J.; Mayes, A. M.; Ross, C. A.; Thomas, E. L.; De Rosa, C. *Appl. Phys. Lett.* **2001**, *79*, 848.
(5) Park, M.; Harrison, C.; Chaikin, P. M.; Register, R. A.; Adamson, D. H. *Science* **1997**, *276*, 1401.
(6) Segalman, R. A. *Mater. Sci. Eng., R* **2005**, *48*, 191.
(7) Thurn-Albrecht, T.; Steiner, R.; DeRouchey, J.; Stafford, C. M.; Huang, E.; Bal, M.; Tuominen, M.; Hawker, C. J.; Russell, T. P. *Adv. Mater.* **2000**, *12*, 1138.
(8) Yang, X.; Xiao, S.; Wu, W.; Xu, Y.; Mountfield, K.; Rottmayer, R.; Lee, K.; Kuo, D.; Weller, D. *J. Vac. Sci. Technol., B* **2007**, *25*, 2202.
(9) Yokoyama, H.; Mates, T. E.; Kramer, E. J. *Macromolecules* **2000**, *33*, 1888.
(10) Bates, F. S.; Fredrickson, G. H. *Annu. Rev. Phys. Chem.* **1990**, *41*, 525.
(11) Bates, F. S.; Fredrickson, G. H. *Phys. Today* **1999**, *52*, 32.
(12) Knoll, A.; Horvat, A.; Lyakhova, K. S.; Krausch, G.; Sevink, G. J. A.; Zvelindovsky, A. V.; Magerle, R. *Phys. Rev. Lett.* **2002**, *89*, 035501.
(13) Liu, Y.; Zhao, W.; Zheng, X.; King, A.; Singh, A.; Rafailovich, M. H.; Sokolov, J.; Dai, K. H.; Kramer, E. J.; et al. *Macromolecules* **1994**, *27*, 4000.
(14) Segalman, R. A.; Hexemer, A.; Hayward, R. C.; Kramer, E. J. *Macromolecules* **2003**, *36*, 3272.
(15) Radzilowski, L. H.; Carvalho, B. L.; Thomas, E. L. *J. Polym. Sci., Part B: Polym. Phys.* **1996**, *34*, 3081.
(16) Konrad, M.; Knoll, A.; Krausch, G.; Magerle, R. *Macromolecules* **2000**, *33*, 5518.
(17) Kim, S. H.; Misner, M. J.; Xu, T.; Kimura, M.; Russell, T. P. *Adv. Mater.* **2004**, *16*, 226.
(18) Edwards, E. W.; Montague, M. F.; Solak, H. H.; Hawker, C. J.; Nealey, P. F. *Adv. Mater.* **2004**, *16*, 1315.
(19) Park, S. M.; Craig, G. S. W.; La, Y. H.; Solak, H. H.; Nealey, P. F. *Macromolecules* **2007**, *40*, 5084.
(20) Daoulas, K. C.; Muller, M.; Stoykovich, M. P.; Park, S. M.; Papakonstantopoulos, Y. J.; de Pablo, J. J.; Nealey, P. F.; Solak, H. H. *Phys. Rev. Lett.* **2006**, 96.
(21) Edwards, E. W.; Stoykovich, M. P.; Muller, M.; Solak, H. H.; De Pablo, J. J.; Nealey, P. F. *J. Polym. Sci., Part B: Polym. Phys.* **2005**, *43*, 3444.
(22) Craig, G. S. W.; Nealey, P. F. *J. Vac. Sci. Technol., B* **2007**, *25*, 1969.
(23) Cheng, J. Y.; Zhang, F.; Chuang, V. P.; Mayes, A. M.; Ross, C. A. *Nano Lett.* **2006**, *6*, 2099.
(24) Thomas, E. L.; Kinning, D. J.; Alward, D. B.; Henkee, C. S. *Macromolecules* **1987**, *20*, 2934.
(25) Edwards, E. W.; Stoykovich, M. P.; Solak, H. H.; Nealey, P. F. *Macromolecules* **2006**, *39*, 3598.
(26) Cheng, J. Y.; Mayes, A. M.; Ross, C. A. *Nat. Mater.* **2004**, *3*, 823.
(27) Walton, D. G.; Kellogg, G. J.; Mayes, A. M.; Lambooy, P.; Russell, T. P. *Macromolecules* **1994**, *27*, 6225.
(28) Turner, M. S. *Phys. Rev. Lett.* **1992**, *69*, 1788.
(29) Park, S. M.; Craig, G. S. W.; Liu, C. C.; La, Y. H.; Ferrier, N. J.; Nealey, P. F. *Macromolecules*, submitted for publication.
(30) Craig, G. S. W.; Nealey, P. F. *J. Photopolym. Sci. Technol.* **2007**, *20*, 511.
(31) Kim, S. O.; Solak, H. H.; Stoykovich, M. P.; Ferrier, N. J.; de Pablo, J. J.; Nealey, P. F. *Nature (London)* **2003**, *424*, 411.
(32) Edwards, E. W.; Muller, M.; Stoykovich, M. P.; Solak, H. H.; de Pablo, J. J.; Nealey, P. F. *Macromolecules* **2007**, *40*, 90.
(33) Henkee, C. S.; Thomas, E. L.; Fetters, L. J. *J. Mater. Sci.* **1988**, *23*, 1685.

MA801039V